Structural Stability and Increase in Size Rationalize the Efficiency of Lipoplexes in Serum

Cristina Marchini,[†] Maura Montani,[†] Augusto Amici,[†] Heinz Amenitsch,[‡] Carlotta Marianecci,[§] Daniela Pozzi,[||] and Giulio Caracciolo*,[||]

Genetic Immunization Laboratory, Department of Molecular Cellular and Animal Biology, University of Camerino, Via Gentile III da Varano, 62032 Camerino (MC), Italy, Institute of Biophysics and Nanosystems Research, Austrian Academy of Sciences, Schmiedelstrasse 6, A-8042 Graz, Austria, Dipartimento di Chimica e Tecnologie del Farmaco, Faculty of Pharmacy, University of Rome "La Sapienza", P. le Aldo Moro 5, 00185 Rome, Italy, and Department of Chemistry, University of Rome "La Sapienza", P. le A. Moro 5, 00185 Rome, Italy

Received October 12, 2008. Revised Manuscript Received November 24, 2008

We have investigated the effect of serum on nanometric structure, size, surface potential, DNA-binding capacity, and transfection efficiency of DDAB-DOPE/DNA and DC-Chol-DOPE/DNA lipoplexes as a function of membrane charge density and cationic lipid/DNA charge ratio. In the absence of serum, the nanometric structure and DNA binding capacity of lipoplexes determined the transfection efficiency. When serum was added, the transfection efficiency of all lipoplex formulations was found to increase. We identified structural stability and an increase in size in serum as major parameters regulating the efficiency of lipofection. By extrapolation, we propose that serum, regulating the size of resistant lipid−DNA complexes, can control the mechanism of internalization of lipoplexes and, in turn, their efficiency.

1. Introduction

Cationic liposomes (CLs) have become widely used as nonviral gene vectors for both in vitro and in vivo applications.[1] Because of their positive charge, they spontaneously associate with negatively charged DNA, thereby forming lipoplexes.[1] Formulations based on the use of zwitterionic lipids and divalent cations have also been investigated.[2]

The ease of cationic lipid synthesis and the availability of lipid technologies resulted in a huge number of lipid transfection reagents. Unfortunately, the absence of supporting biology of transfection resulted in plateauing of transfection efficiencies by lipoplexes. As a result, understanding the mechanisms of lipid-mediated delivery is definitely more compelling now.

Among the barriers to transfection, serum has been reported to exert its inhibitory effect.[3−6] Serum components interact with the lipoplex in a nonspecific manner. Two kinds of effects of serum have been reported. First, serum proteins such as albumin, lipoproteins, fibrinogen, and heparin can bind to lipid membranes, causing aggregation of lipoplexes and resulting in size increases and decreases as a function of the zeta potential.[4,5] As a result, the interaction of lipoplexes with the cell or the interaction of DNA with the cationic lipid is weakened. The second effect is a destabilization of the lipoplex structure, which may induce the dissociation of DNA from the complexes. Lipoplexes can be arranged into lamellar or inverted hexagonal phases (Figure 1) depending on lipid composition. A serum-induced lamellar-to-hexagonal phase transition of lipid membranes has been also proposed[6] but, to the best of our knowledge, has not been reported so far.

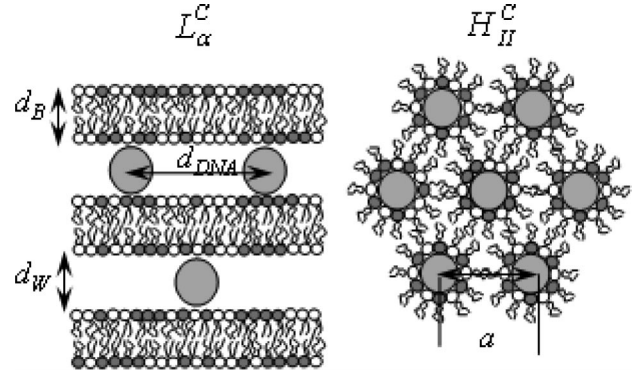

Figure 1. Schematics of the inner structure of lamellar and hexagonal CL-DNA complexes. The lamellar phase, L_α^C, is composed of alternative lipid bilayers and DNA monolayers, with the repeat spacing given by $d = d_W + d_B$. The hexagonal phase, H_{II}^C, is composed of cylinders consisting of DNA coated with a lipid monolayer arranged on a hexagonal lattice.

The presence of serum at the time of lipoplex incubation with cells, in general, was found to decrease the transfection,[7−9] hence the desire to develop formulations of lipoplexes that are unaffected

* To whom correspondence should be addressed. Tel: +39 06 4991 3076. Fax: +39 06 490631. E-mail: g.caracciolo@caspur.it.
[†] University of Camerino.
[‡] Austrian Academy of Sciences.
[§] Dipartimento di Chimica e Tecnologie del Farmaco, University of Rome "La Sapienza".
[||] Department of Chemistry, University of Rome "La Sapienza".

(1) Felgner, P. L.; Ringold, G. M. *Nature* **1989**, *331*, 461–462.
(2) McManus, J.; Rädler, J. O.; Dawson, K. A. *Langmuir* **2003**, *19*, 9630–9637.
(3) Yang, J. P.; Huang, L. *Gene Ther.* **1997**, *4*, 950–960.
(4) Zelphati, O.; Uyechi, L. S.; Barron, L. G.; Szoka, F. C., Jr. *Biochim. Biophys. Acta* **1998**, *1390*, 119–133.
(5) Simberg, D.; Weisman, S.; Talmon, Y.; Faerman, A.; Shoshani, T.; Barenholz, Y. *J. Biol. Chem.* **2003**, *278*, 39858–39865.
(6) Wasungu, L.; Scarzello, M.; van Dam, G.; Molema, G.; Wagennar, A.; Engberts, J. B. F. N.; Hoekstra, D. *J. Mol. Med.* **2006**, *84*, 774–784.
(7) Vitiello, L.; Bockhold, K.; Joshi, P. B.; Worton, R. G. *Gene Ther.* **1998**, *5*, 1306–1313.
(8) Wasan, E. K.; Harvie, P.; Edwards, K.; Karlsson, G.; Bally, M. B. *Biochim. Biophys. Acta* **1999**, *1461*, 27–46.
(9) Turek, J.; Dubertret, C.; Jaslin, G.; Antonakis, K.; Scherman, D.; Pitard, B. *J. Gene Med.* **2000**, *2*, 32–40.

10.1021/la8033726 CCC: $40.75
Published on Web 02/05/2009

by serum.[10] Unfortunately, the mechanisms that regulate the stability of lipoplexes in serum as well as the details of lipoplex−serum interaction are still poorly understood.

The present work is intended to investigate the effect of fetal bovine serum (FBS) on the colloidal stability (structure, size, zeta potential, and DNA-binding capacity) of lipoplexes and to try to correlate it with transfection efficiency (TE). Because of the amphiphile-dependent nature of the interaction of lipoplexes with serum proteins, we prepared different lipoplex formulations by fixing the neutral helper lipid (DOPE) but varying the cationic lipid (by incorporating DDAB or DC-Chol in the binary mixtures). Some authors have suggested that serum stability may be dependent on the membrane charge density of lipoplexes.[11,12] To test this suggestion, we maintained a constant quantity of the cationic lipid (alternatively DDAB or DC-Chol) and varied the amount of DOPE within the formulation.

Structural changes of lipoplexes in serum were investigated by means of high-resolution synchrotron small-angle X-ray scattering (SAXS). The effect of serum on the size of the complexes was assessed by dynamic light scattering (DLS), whereas the association between lipid and DNA in serum was evaluated by agarose gel electrophoresis. These physicochemical properties were compared with the transfection of NIH 3T3 cells. Despite most previous results,[7−9] the transfection efficiency of all lipoplex formulations was found to increase in the presence of FBS. Lipoplexes were stable in serum, and no appreciable changes in lamellar structure and DNA packing density were detected. DNA was not released from the lipoplexes, and the morphology of DNA protected by cationic lipids was not affected by serum. On the contrary, major changes in lipoplex size in the presence of serum were detected. According to the accepted size-dependent entry mechanism of lipoplexes, our results seemingly suggest that the increase in transfection efficiency in serum may be likely due to a serum-induced switch from a clathrin-dependent to a caveolae-mediated mechanism of lipoplex internalization.

2. Materials and Methods

2.1. Cationic Liposome Preparation. Cationic 1,2-dioleoyl-3-trimethylammonium-propane (DOTAP), dimethyldioctadecylammonium bromide (DDAB), (3β-[*N*-(*N*′,*N*′-dimethylaminoethane)-carbamoyl])-cholesterol (DC-Chol) and neutral dioleoylphosphatidylethanolamine (DOPE) were purchased from Avanti Polar Lipids (Alabaster, AL) and used without further purification. DDAB-DOPE and DC-Chol-DOPE cationic liposomes were prepared according to standard protocols.[13] In brief, each binary mixture, at a molar fraction of neutral lipid in the bilayer of Φ = (neutral lipid/total lipid) (mol/mol) = 0.5 and 0.7, was dissolved in chloroform, and the solvent was evaporated under vacuum for at least 24 h. The obtained lipid films were hydrated with the appropriate amount of Tris-HCl buffer solution (10^{-2} M, pH 7.4) to achieve the desired final concentration (10 mg/mL for the X-ray samples). The obtained liposome solutions were sonicated to clarity and stored at 30 °C for 48 h to achieve full hydration.[14]

2.2. Lipoplex Preparation. Calf thymus Na-DNA was purchased from Sigma-Aldrich (St. Louis, MO). DNA was dissolved in Tris-HCl buffer (5 mg/ml) and was sonicated for 5 min, inducing DNA fragmentation with a length distribution between 500 and 1000 base pairs, which was determined by gel electrophoresis. Plasmid DNA (pGL3, which codes for firefly luciferase) was purchased from Promega (Madison, WI). By mixing adequate amounts of the DNA solutions in suitable volumes of liposome dispersions, self-assembled DDAB-DOPE/DNA and DC-Chol-DOPE/DNA binary lipoplexes were obtained. After 20 min of incubation, DMEM was added to the lipoplex dispersion to obtain the final concentration. Furthermore, all samples were prepared with several cationic lipid/DNA ratios (mol/mol) (i.e., ρ = (cationic lipid (by mole)/DNA base) = 0.5, 1, 2.5, 3, 5). Lipoplexes in serum were formed according to the following protocol. First, lipoplexes were allowed to form for 24 h. The lipoplex suspension was subsequently diluted in buffer with serum (50% vol/vol). Diluting serum with an equal volume of buffer approximates the physiological serum concentration.[15] Such lipoplexes are indicated in the subsequent text as FBS lipoplexes. Samples were stored for 3 days at 4 °C.[14]

2.3. Transfection Efficiency Experiments. Cell lines were cultured in Dulbecco's modified Eagle's medium (DMEM) (Invitrogen, Carlsbad, CA) supplemented with 1% penicillin−streptomycin (Invitrogen) and 10% fetal bovine serum (FBS, Invitrogen) at 37 °C in a 5% CO_2 atmosphere, splitting the cells every 2−4 days to maintain monolayer coverage. For luminescence analysis, mouse fibroblast NIH 3T3 cells were transfected with pGL3 control plasmid (Promega). The day before transfection, cells were seeded in 24-well plates (150 000 cells/well) using a medium without antibiotics. Cells were incubated until they were 75−80% confluent, which generally took 18 to 24 h. For TE experiments, lipoplexes were prepared by mixing 0.5 μg of plasmid with 5 μL of sonicated lipid dispersions (1 mg/mL) for each well. These complexes were allowed to form for 20 min, and lipoplexes were subsequently diluted in DMEM or in DMEM/serum (50% vol/vol) and left for 20 min at room temperature before adding them to the cells. The cells were incubated with lipoplexes in Optimem (Invitrogen) for 6 h to permit transient transfection; the medium was then replaced with DMEM supplemented with FBS. Luciferase expression was analyzed after 48 h and measured with the luciferase assay system from Promega, and light output readings were performed on a Berthold AutoLumat luminometer LB-953 (Berthold, Bad Wildbad, Germany). TE was normalized to milligrams of total cellular protein in the lysates using the Bio-Rad protein assay dye reagent (Bio-Rad, Hercules, CA).

2.4. Synchrotron Small-Angle X-ray Scattering Measurements. Small-angle X-ray scattering (SAXS) measurements were carried out at the ID2 high-brilliance beamline at the European Synchrotron Radiation Facility (Grenoble, France). The energy of the incident beam was 12.5 KeV (λ = 0.995 Å), the beam size was 100 μm, and the sample-to-detector distance was 1.2 m. The diffraction patterns were collected with a 2D CCD detector (Frelon Camera). We investigated the q range from q_{min} = 0.04 Å^{-1} to q_{max} = 0.5 Å^{-1} with a resolution of 5×10^{-4} Å^{-1} (fwhm). The sample was held in a 1 mm glass capillary (Hildberg, Germany). Measurements were performed at 25 °C. To avoid radiation damage, a maximum exposure time of 3 s/frame was used for any given sample. Satisfactory statistics were obtained by repeating several measurements on fresh samples. The collected 2D powder diffraction spectra were angularly integrated using the FIT2D package. These data were then corrected for the detector efficiency, empty sample holder, and bulk solution.

2.5. Small-Angle X-ray Scattering Data Analysis. Bragg peak positions, widths, and intensities of some diffraction patterns were analyzed by multiple fitting of Lorentzian distributions.[16] Structural parameters of lipid bilayers (i.e., the bilayer thickness, d_B, and the water layer thickness, d_W) were calculated by standard procedures (i.e., the electron density profile was deduced from the diffraction data). For further details, see the protocols given in refs 17−19.

2.6. Size and Zeta Potential Measurements. All sizing and zeta potential measurements were made on a Zetasizer Nano ZS90 (Malvern, U.K.) at 25 °C with a scattering angle of 90.0°. Sizing measurements were made on the neat vesicle dispersions, whereas the samples were diluted 1/10 with distilled water for the zeta potential

(10) Audouy, S.; Molema, G.; de Leij, L.; Hoekstra, D. *J. Gene Med.* **2000**, *2*, 465–476.
(11) Zhang, Y.; Anchordoquy, T. J. *Biochim. Biophys. Acta* **2004**, *1663*, 143–157.
(12) Simberg, D.; Weiss, A.; Barenholz, Y. *Hum. Gene Ther.* **2005**, *16*, 1087–1096.
(13) Caracciolo, G.; Pozzi, D.; Caminiti, R.; Amenitsch, H. *Langmuir* **2005**, *21*, 11582–11587.
(14) Pozzi, D.; Amenitsch, H.; Caminiti, R.; Caracciolo, G. *Chem. Phys. Lett.* **2006**, *429*, 250–254.
(15) Templeton, N. S. *Curr. Med. Chem.* **2003**, *10*, 1279–1287.
(16) Luzzati, V.; Mariani, P.; Delacroix, H. *Makromol. Chem., Macromol. Symp.* **1998**, *15*, 1–17.

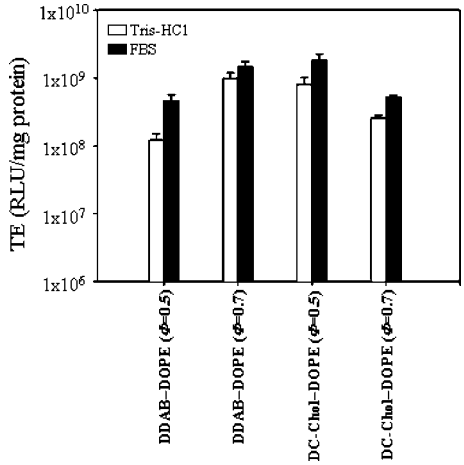

Figure 2. Transfection efficiency in RLU/mg of cellular proteins of DDAB-DOPE/DNA ($\Phi = 0.5$), DDAB-DOPE/DNA ($\Phi = 0.7$), DC-Chol-DOPE/DNA ($\Phi = 0.5$), and DC-Chol-DOPE/DNA ($\Phi = 0.7$) lipoplexes in the absence (white histograms) and in the presence of serum (black histograms).

experiments to obtain reliable and accurate measurements. For all samples investigated, the data show a unimodal distribution and represent the average of at least five different measurements carried out for each sample. The polydispersity index (pdi) was directly calculated by the software of the apparatus.

2.7. Agarose Gel Electrophoresis Experiments. Electrophoresis studies were conducted on 1% agarose gels containing ethidium bromide in Tris-borate-EDTA (TBE) buffer. Lipoplexes were prepared by mixing 42 μL of lipid dispersions with 5.4 μg of pGL3 control plasmid. These complexes were allowed to equilibrate for 30 min at room temperature before adding 42 μL of Tris-HCl buffer or 42 μL of FBS. After 30 min, lipoplexes, lipoplexes plus serum, naked plasmid DNA, and naked plasmid DNA plus serum were analyzed by electrophoresis. For this purpose, 10 μL of each sample was mixed with 2 μL of loading buffer (glycerol 30%, bromophenol blue 0.25%) and subjected to agarose gel electrophoresis for 1 h at 80 V. The electrophoresis gel was visualized and digitally photographed using a Kodak Image Station, model 2000 R (Kodak, Rochester, NY). Digital photographs were enhanced using dedicated software (Kodak MI, Kodak) that allows the calculation of the molar fraction of released DNA, X_{DNA}.

To demonstrate that serum has a degradative effect on free DNA (not complexed with lipids) but not on DNA inside the lipoplexes and to evaluate the presence of DNA inside the lipoplex, the different samples were subjected to phenol−chloroform extraction. To isolate DNA, equal volumes of a phenol/chloroform mixture and the aqueous sample were mixed, forming a biphasic mixture upon centrifugation with an upper aqueous phase and a precipitated organic phase. The aqueous phase with nucleic acids was recovered, and DNA was precipitated with Na-acetate/ethanol and resuspended in 74 μL of Tris-HCl. Finally, 10 μL of each sample was subjected to gel electrophoresis.

3. Results

3.1. Transfection Efficiency Results. The transfection activity of lipoplexes prepared in a serum-free cell culture medium was tested in vitro using luciferase expression in the mouse fibroblast NIH 3T3 cell line. The results are presented in Figure 2 (white histograms). The transfection efficacy of DDAB-DOPE/DNA ($\Phi = 0.5$) lipoplexes was the lowest of the four formulations. The transfection efficiencies of DDAB-DOPE/DNA ($\Phi = 0.7$) and DC-Chol-DOPE/DNA ($\Phi = 0.5$) lipoplexes were the highest and virtually identical, whereas DC-Chol-DOPE/DNA ($\Phi = 0.5$) complexes exhibited an intermediate value.

In the presence of serum, the transfection efficiency of all lipoplex formulations increased (black histograms) with increasing TE(serum)/TE(buffer) ratio, varying between 1.5 for DDAB-DOPE/DNA at $\Phi = 0.7$ and 3.7 for DDAB-DOPE/DNA at $\Phi = 0.5$. DC-Chol-DOPE/DNA lipoplexes had intermediate increasing ratios. This was a very unusual result because the presence of serum at the time of lipoplex incubation with the cells has been mostly found to decrease the transfection efficiency.[7−9] In our search for the reason that the transfection efficiency of lipoplexes increased in the presence of FBS, we investigated the effect of serum on the structure, size, zeta potential, and DNA-protection capacity of lipoplexes. Physical−chemical properties of lipoplexes were therefore characterized in the absence and in the presence of serum.

3.2. Structure of Lipoplexes. The structure of DC-Chol-DOPE/DNA and DDAB-DOPE/DNA lipoplexes in the absence and in the presence of serum has recently been investigated by means of in-house diffraction experiments,[20] but the phase and DNA packing density of lipoplexes were not clearly characterized because of the extremely low experimental resolution. In this work, we took specific advantage of using very brilliant synchrotron radiation. As a result, synchrotron SAXS experiments revealed the nanostructure of lipoplexes unambiguously. All lipoplexes were arranged in lamellar arrays (lamellar L_α^C phase, Figure 1). Figure 3 (panel a) shows a set of representative synchrotron SAXS patterns of DC-Chol-DOPE/DNA lipoplexes at $\Phi = 0.5$ and increasing ρ (from the bottom to the top). X-ray patterns showed sharp peaks at $q_{001} = 0.091$ Å^{-1}, $q_{002} = 0.182$ Å^{-1}, $q_{003} = 0.273$ Å^{-1}, and $q_{005} = 0.456$ Å^{-1} (the 004 reflection is absent owing to the form factor)[14] resulting from the layered structure of the L_α^C phase ($d = d_B + d_W = 2\pi/q_{001} = 68.9$ Å) with DNA intercalated between cationic lipid bilayers (Figure 1). For DC-Chol-DOPE/DNA lipoplexes at $\Phi = 0.7$, SAXS patterns (Figure 3, panel b) revealed five orders of Bragg peaks at $q_{001} = 0.089$ Å^{-1}, $q_{002} = 0.178$ Å^{-1}, $q_{003} = 0.266$ Å^{-1}, $q_{004} = 0.356$ Å^{-1}, and $q_{005} = 0.455$ Å^{-1} denoting a repeat spacing of $d = 70.6$ Å.

Whereas the lamellar (001) peaks do not move with ρ, the much broader and weaker peak arising from the DNA−DNA correlations[21,22] (solid arrows) shifts with changes in ρ and Φ. This can be seen in Figure 3 (panel c), where d_{DNA} changes with ρ from 29.4 to 31.9 Å at $\Phi = 0.5$ (●) and from 39.3 to 41.4 Å at $\Phi = 0.7$ (△). It has been recently proposed[20] that the high efficacy of DC-Chol-DOPE/DNA lipoplexes is likely related to their inverted hexagonal phase. Conversely, high-resolution synchrotron SAXS experiments reported here show that DC-Chol-DOPE/DNA lipoplexes are lamellar over a wide compositional range of lipid composition.

Figure 4 shows representative synchrotron SAXS patterns of DDAB-DOPE/DNA lipoplexes at $\Phi = 0.5$ (panel a) and $\Phi = 0.7$ (panel b) with increasing ρ (from bottom to top). In either case, we observe a set of equally spaced (00l) Bragg reflections arising from the lamellar membrane repeat distance ($d = 67.4$ and 70.7 Å at $\Phi = 0.5$ and 0.7, respectively). SAXS patterns of DDAB-DOPE/DNA lipoplexes at $\Phi = 0.7$ (panel b) also show a second set of peaks, which is consistent with a 2D columnar inverted hexagonal structure where the DNA strands are surrounded by a lipid monolayer with the DNA−lipid inverted

(17) Francescangeli, O.; Rinaldi, D.; Laus, M.; Galli, G.; Gallot, B. *J. Phys. II* **1996**, *6*, 77–89.
(18) Zantl, R.; Baicu, L.; Artzner, F.; Sprenger, I.; Rapp, G.; Rädler, J. O. *J. Phys. Chem. B* **1999**, *103*, 10300–10310.
(19) Caracciolo, G.; Pozzi, D.; Amenitsch, H.; Caminiti, R. *Langmuir* **2006**, *22*, 4267–4273.
(20) Esposito, C.; Generosi, J.; Mossa, G.; Masotti, A.; Congiu Castellano, A. *Colloids Surf. B* **2006**, *53*, 187–192.
(21) Caracciolo, G.; Caminiti, R. *Chem. Phys. Lett.* **2005**, *400*, 314–319.
(22) Caracciolo, G.; Pozzi, D.; Caminiti, R.; Marchini, C.; Montani, M.; Amici, C.; Amenitsch, H. *J. Phys. Chem. B* **2008**, *112*, 11298–11304.

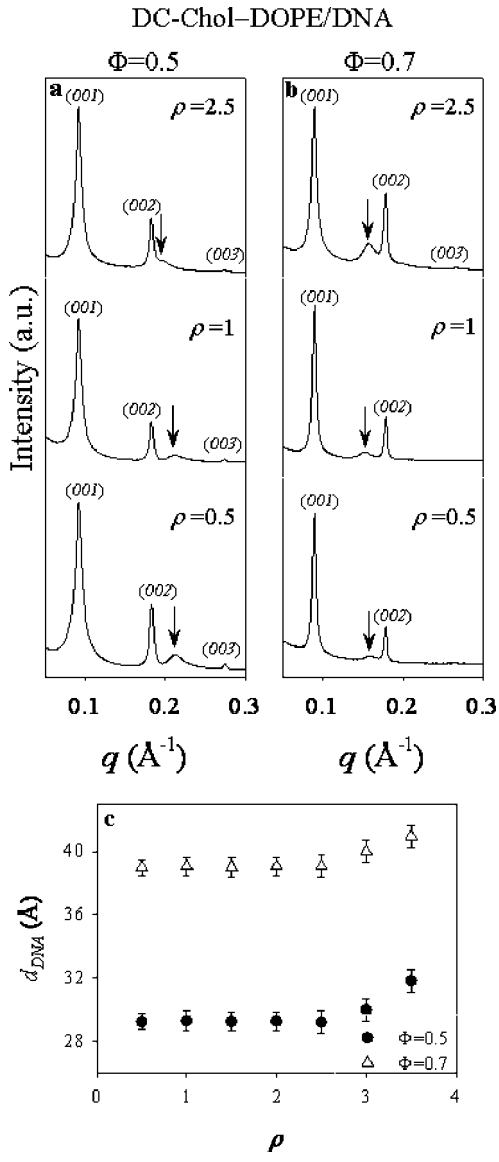

Figure 3. (a) Representative synchrotron SAXS patterns of DC-Chol-DOPE/DNA lipoplexes at $\Phi = 0.5$ as a function of increasing ρ (from bottom to top). The interhelical DNA−DNA distance peak is marked by an arrow. (b) Synchrotron SAXS patterns of DC-Chol-DOPE/DNA lipoplexes at $\Phi = 0.7$ as a function of increasing ρ (from the bottom to the top). (c) DNA interdistance, d_{DNA}, as a function of ρ for DC-Chol-DOPE/DNA lipoplexes at $\Phi = 0.5$ (●) and $\Phi = 0.7$ (△). For clarity, the q range is restricted to 0.05−0.3 Å^{-1}.

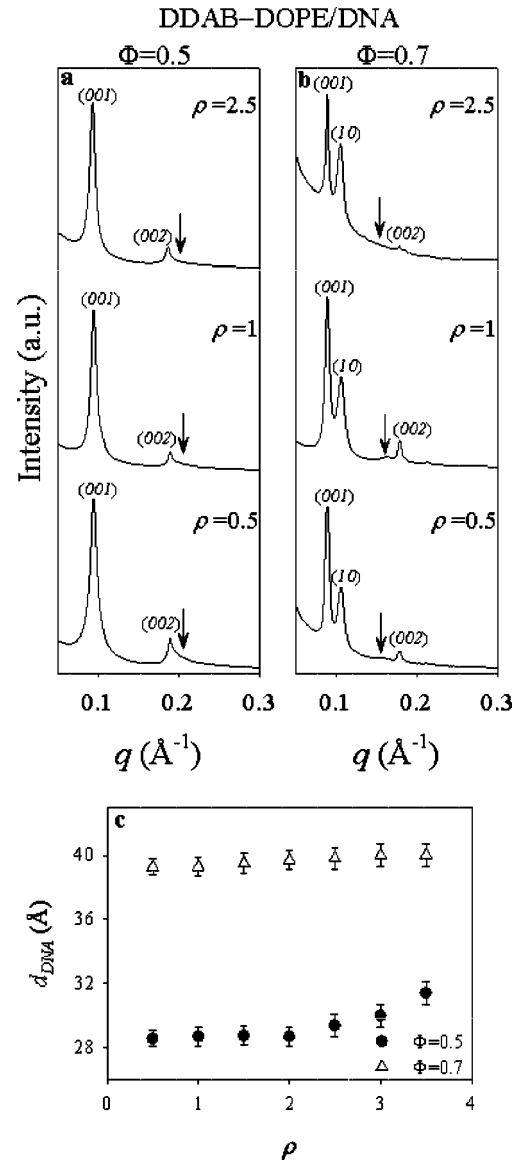

Figure 4. (a) Representative synchrotron SAXS patterns of DDAB-DOPE/DNA lipoplexes at $\Phi = 0.5$ as a function of increasing ρ (from bottom to top). The interhelical DNA−DNA distance peak is marked with an arrow. (b) Synchrotron SAXS patterns of DDAB-DOPE/DNA lipoplexes at $\Phi = 0.7$ as a function of increasing ρ (from bottom to top). (c) DNA interdistance, d_{DNA}, as a function of ρ for DDAB-DOPE/DNA lipoplexes at $\Phi = 0.5$ (●) and $\Phi = 0.7$ (△).

cylindrical micelles arranged on a hexagonal lattice (Figure 1). In the present study, we observed Bragg peaks up to seventh order, which indicates a high degree of regularity of the structure. Diffraction peaks could be indexed perfectly on a 2D hexagonal lattice with a unit cell spacing of $a = 68.2$ Å according to the equation $q_{hk} = (4\pi)/(\sqrt{3}a)\sqrt{h^2 + hk + k^2}$. Such a structure resembles that of the inverted hexagonal H_{II} phase of pure DOPE in excess water and has already been observed in DOPE-containing lipoplexes.[13,23,24] The coexistence of these two lipid geometries has already been reported[13,23,24] and is dictated by a critical interplay between the membrane charge density and the elastic properties of the constituent lipid bilayers.[23] We show in Figure 4 (panel c) a set of $d_{DNA}(\rho)$ curves for DDAB-DOPE/DNA lipoplexes with $\Phi = 0.5$ (●) and $\Phi = 0.7$ (△).

With the aim of providing all of the relevant structural parameters, electron density profiles along the normal to lipid bilayers were calculated from the SAXS patterns of Figures 3 and 4. In Figure 5, a comparison between the profiles of DC-Chol-DOPE/DNA lipoplexes at $\Phi = 0.5$ (−) and DC-Chol-DOPE/DNA lipoplexes at $\Phi = 0.7$ (•••) is shown. The EDPs of Figure 5 show the usual lipid bilayer density plus high-density regions at the outer edges of the profile due to the DNA rod lattices intercalated between opposing bilayers. The more electron dense regions (i.e., the two maxima in the electron density profiles of Figure 5) represent the headgroup region, and the pronounced central minimum at $z = 0$ corresponds to the terminal methyl groups of the opposing acyl chains. According to recent models,[25] the distance between the maxima plus the fwhm of the Gaussian representing a polar headgroup provides a reasonable estimate

(23) Koltover, I.; Salditt, T.; Rädler, J. O.; Safinya, C. R. *Science* **1998**, *281*, 78–81.

(24) Caracciolo, G.; Pozzi, D. Caminiti; Amenitsch, H. *Appl. Phys. Lett.* **2007**, *91*, 143903–3.

(25) Pabst, G.; Rappolt, M.; Amentisch, H.; Laggner, P. *Phys. Rev. E* **2000**, *62*, 4000–4009.

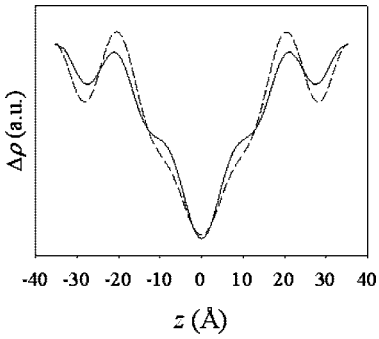

Figure 5. Electron density profiles along the normal to the bilayers of DC-Chol-DOPE/DNA lipoplexes at $\Phi = 0.5$ (−) and at $\Phi = 0.7$ (•••).

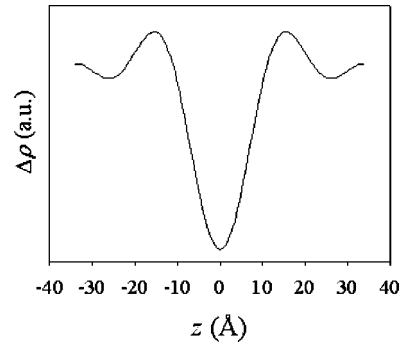

Figure 6. Electron density profile of the hexagonal phase of DDAB-DOPE/DNA lipoplexes at $\Phi = 0.7$.

Table 1. Lamellar Periodicity, *d*, Lipid Bilayer Thickness, d_B, and Thickness of the Interbilayer Water Region, d_W, of DC-Chol-DOPE/DNA and DDAB-DOPE/DNA Lipoplexes

	DC-Chol-DOPE/DNA		DDAB-DOPE/DNA		
	$\Phi = 0.5$	$\Phi = 0.7$	$\Phi = 0.5$	$\Phi = 0.7$	
	L_α^C	L_α^C	L_α^C	L_α^C	H_{II}^C
D	68.9	70.8	67.4	70.7	68.3
d_B	47.6	51.3	n.d.[a]	46.6	40.9
d_W	21.3	19.5	n.d.[a]	24.1	27.4

[a] n.d. means not detected.

of the membrane thickness, d_B. According to general definitions,[25] the lamellar repeat distance d is the sum of the membrane thickness, d_B, and the water layer thickness, d_W (Figure 1). Thus, the interbilayer water thickness is usually defined as $d_W = d - d_B$.

In Figure 5, we observe that changing the composition of the lipid bilayer results in a more pronounced maximum in electron density with increasing Φ. A molecular interpretation can be given if the difference in the chemical structure of the lipids is considered. Indeed, the headgroup of DOPE exhibits a higher electron density than that of DC-Chol, and it produces stronger maxima in the EDP. All calculated structural parameters of DC-Chol-DOPE/DNA lipoplexes are reported in Table 1. Note that the spatial extension of the lipid headgroup region, d_H, estimated from the fwhm of the Gaussian maxima of the EDPs increases with Φ from 7.5 at $\Phi = 0.5$ to ∼10 Å at $\Phi = 0.7$. These findings are in very good agreement with those reported in the literature for DOPE and DOPE/Chol mixtures.[26] Furthermore, we observed that membrane thickness varied from 47.9 Å at $\Phi = 0.5$ to 51.2 Å at $\Phi = 0.7$. Such swelling depends on the fact that the DOPE molecule is longer than DC-Chol and the headgroup area (and therefore the bilayer thickness) of the lipids may vary slightly to accommodate the projected area/anionic group of the DNA molecule.

In the SAXS patterns of DDAB-DOPE/DNA lamellar lipoplexes at $\Phi = 0.5$ (Figure 4, panel a), just the first- and second-order Bragg peaks of the lamellar phase were detected. As a consequence, a detailed EDP could not be calculated. Conversely, the two peak sets detected on the SAXS pattern of DDAB-DOPE/DNA lamellar lipoplexes at $\Phi = 0.7$ (Figure 4, panel b) allowed us to calculate detailed EDPs of both the lamellar and the hexagonal phases from which structural parameters were calculated (Table 1). In Figure 6, we show the EDP of the hexagonal phase of DDAB-DOPE/DNA lipoplexes at $\Phi = 0.7$ calculated as explained in ref 27.

The in-plane packing of the hydrocarbon chains was evaluated by WAXS experiments (not reported). The WAXS broad peak ($1.2 < q < 1.6$ Å^{-1}) with a corresponding d value of about 4.5 Å provides evidence that lipid membranes of all lipoplex formulations are in the fluid liquid-crystalline state.

3.3. Effect of Serum on the Structure of Lipoplexes. The stability of lipoplexes in the presence of serum can be regarded as a first approximation to gain insight into the behavior of such lipid-based carriers in biological fluids. Thus, synchrotron SAXS was used to investigate the effect of serum on the nanostructure of lipoplexes. Figure 7 (panel a) shows representative synchrotron SAXS patterns of DC-Chol-DOPE/DNA-FBS lipoplexes at $\Phi = 0.5$ and increasing ρ (from bottom to top). Sharp peaks were detected at $q_{001} = 0.089$ Å^{-1}, $q_{002} = 0.177$ Å^{-1}, $q_{003} = 0.266$ Å^{-1}, $q_{004} = 0.356$ Å^{-1}, and $q_{005} = 0.443$ Å^{-1} resulting from the layered structure of the L_α^C phase ($d = 71.1$ Å) with DNA intercalated between cationic lipid bilayers ($d_{DNA} = 30.6$ Å). Neither the lamellar repeat spacing, d, nor the DNA−DNA correlation, d_{DNA}, of lipoplexes in serum varied appreciably with ρ. Also, DC-Chol-DOPE/DNA-FBS lipoplexes at $\Phi = 0.7$ maintained their lamellar structure ($d = 71.6$ Å) in the presence of serum as shown by SAXS patterns of Figure 7 (panel b).

EDPs were calculated from the SAXS patterns of Figure 7, and structural parameters are listed in Table 2. The addition of serum to DC-Chol-DOPE/DNA lipoplexes produced two main effects: (i) Lamellar structure was preserved with a slight enlargement of lamellar d spacing (less than 2 Å). Recent studies showed that cationic lipid vectors recruit large amounts of serum proteins, particularly those containing DOPE as a helper lipid.[28] Thus, the observed swelling of DC-Chol-DOPE membranes is most likely due to serum protein intercalation within lipid bilayers.[3,4] (ii) The DNA packing density remain roughly unaltered, suggesting that DNA was not released from lipoplexes upon interaction with serum.[29,30] The latter observation most likely suggests that serum components did not penetrate into water layers occupied by DNA molecules but appeared to be associated mainly with the lipid membranes.

The addition of serum to DDAB-DOPE/DNA lipoplexes at $\Phi = 0.5$ produced major structural modifications in the lipoplex structure. SAXS patterns (Figure 8, panel a) show the coexistence of lamellar and hexagonal phases. This finding suggests that serum component binding to lipid membranes can modulate the lipid packing and, in turn, promote the phase transition of lipid membranes. It has been recently hypothesized that serum protein

(26) Chen, Z.; Rand, R. P. *Biophys. J.* **1997**, *73*, 267–276.
(27) Fancescangeli, O.; Pisani, M.; Stanić, V.; Bruni, P.; Weiss, T. M. *Europhys. Lett.* **2004**, *67*, 669–675.
(28) Li, S.; Rizzo, M. A.; Bhattacharya, S.; Huang, L. *Gene Ther.* **1998**, *5*, 930–937.
(29) Caracciolo, G.; Pozzi, D.; Caminiti, R.; Marchini, C.; Montani, M.; Amici, A.; Amenitsch, H. *Appl. Phys. Lett.* **2006**, *89*, 233903–3.
(30) Caracciolo, G.; Pozzi, D.; Caminiti, R.; Amenitsch, H. *Langmuir* **2007**, *23*, 8713–8717.

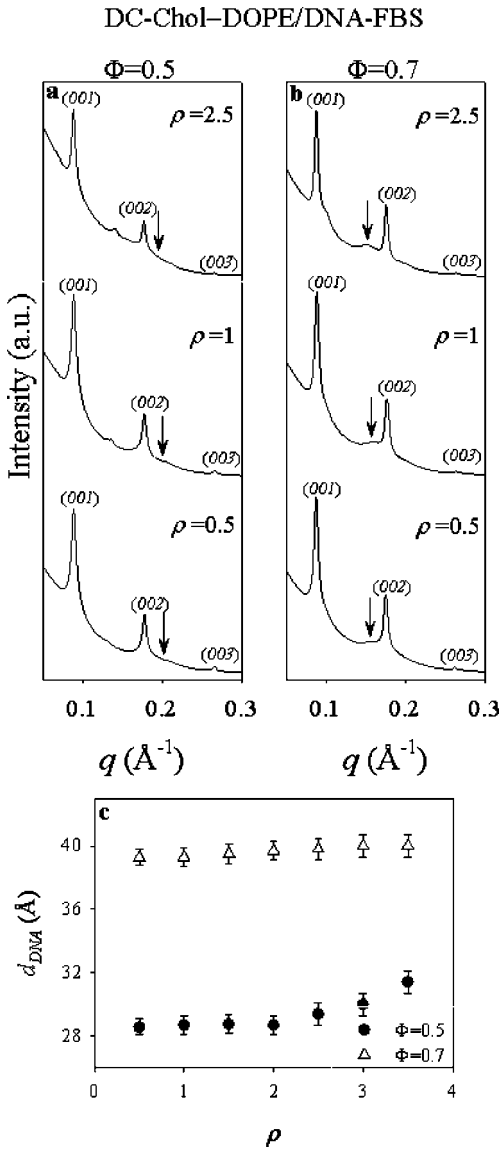

Figure 7. Synchrotron SAXS patterns of DC-Chol-DOPE/DNA-FBS lipoplexes at (a) $\Phi = 0.5$ and (b) $\Phi = 0.7$. (c) DNA interdistance, d_{DNA}, as a function of ρ ($\Phi = 0.5$ (●) and 0.7 (△)).

Table 2. Lamellar Periodicity, *d*, Lipid Bilayer Thickness, d_B, and Thickness of the Interbilayer Water Region, d_W, of DC-Chol-DOPE/DNA-FBS and DDAB-DOPE/DNA-FBS Lipoplexes

	DC-Chol-DOPE/DNA-FBS		DDAB-DOPE/DNA-FBS			
	$\Phi = 0.5$	$\Phi = 0.7$	$\Phi = 0.5$		$\Phi = 0.7$	
	L_α^C	L_α^C	L_α^C	H_{II}^C	L_α^C	H_{II}^C
d	71.1	71.6	69.4	71.5	71.3	68.5
d_B	51.5	51.8	46.9	43.8	50.7	42.4
d_W	19.6	19.8	22.5	27.7	20.6	26.1

intercalation within lipid bilayers can promote the formation of nonlamellar motifs in the membrane of lipoplexes.[6] However, to the best of our knowledge, such a phase transition has not been reported so far. The lamellar *d* spacing ($d = 69.4$ Å) of DDAB-DOPE/DNA-FBS lipoplexes at $\Phi = 0.5$ was about 2 Å larger than for their counterpart in aqueous solution. This finding resembles the swelling behavior of DC-Chol-DOPE/DNA-FBS lipoplexes.

At $\Phi = 0.7$, DDAB-DOPE/DNA-FBS lipoplexes show the coexistence of lamellar and hexagonal phases as observed in the absence of serum (Figure 4, panel b). Both lamellar and hexagonal phases swelled in the presence of serum. Because phase coexistence was also observed in the absence of serum (Figure 4, panel b), it may be difficult to prove whether a serum-induced lamellar-to-hexagonal phase transition was observed in the case of DDAB-DOPE/DNA-FBS lipoplexes at $\Phi = 0.5$. The intensity ratio between the first-order peaks of the lamellar and the hexagonal phases, $R = I_{L(001)}/I_{H(10)}$ changed from $R \approx 5$ in buffer to $R \approx 2.5$ in the presence of serum. This ratio was found to be poorly dependent on the charge ratio of lipoplexes. Aside from being a quantitative analysis, the ratio between Bragg peak intensities is often used as an indicator of phase transitions in lipid systems. Thus, the variation in the intensity ratio at $\Phi = 0.7$ most likely supports our suggestion on the phase evolution of DDAB-DOPE/DNA lipoplexes in the presence of serum.

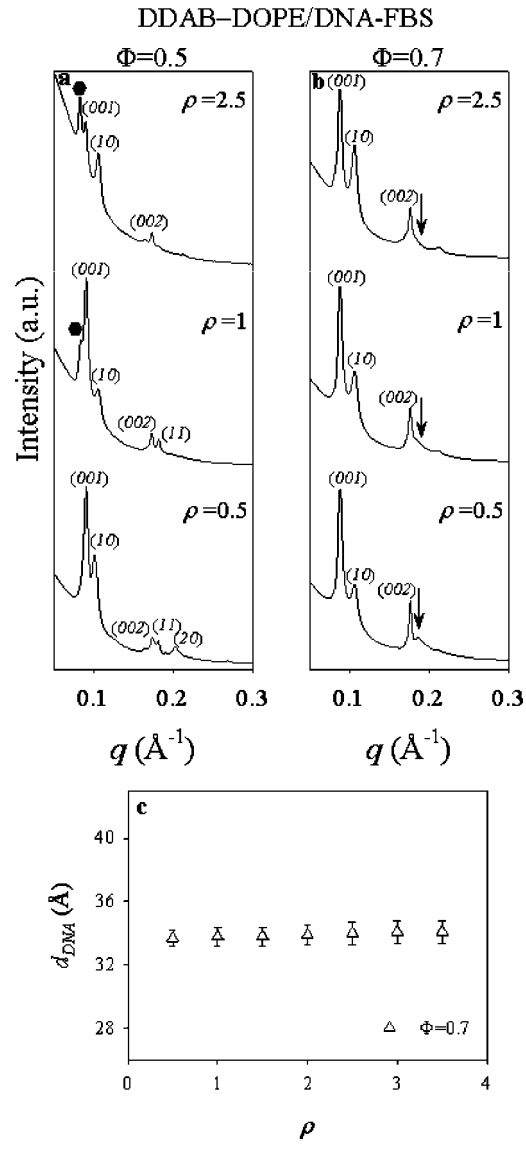

Figure 8. Synchrotron SAXS patterns of DDAB-DOPE/DNA-FBS lipoplexes at (a) $\Phi = 0.5$ and (b) 0.7. (c) DNA interdistance, d_{DNA}, as a function of ρ ($\Phi = 0.5$ (●) and 0.7 (△)). At $\Phi = 0.5$, charge-neutral ($\rho = 1$) and positively charged lipoplexes ($\rho > 1$) start to coexist with pure lipids (⬢).

3.4. Effect of Serum on the Size of Liposomes. The size of the four selected cationic liposome formulations was examined by dynamic light scattering both in the presence and absence of serum. Table 3 shows the mean diameters of liposomes employed in this study. Most vesicles are close to 100 nm in diameter.

Table 3. Size, *D*, and ζ Potential, ζ_P, of Liposomes and Lipoplexes in the Absence and in the Presence of Fetal Bovine Serum (FBS)

liposome formulation	Φ	*D* (nm)	ζ_P (mV)
DDAB-DOPE	0.5	116 ± 1	62.7 ± 1.2
DDAB-DOPE-FBS		434 ± 7	−8.8 ± 0.5
DDAB-DOPE/DNA		368 ± 16	46.6 ± 0.5
DDAB-DOPE/DNA-FBS		734 ± 34	−25.2 ± 0.3
DC-Chol-DOPE		109 ± 2	56.3 ± 1.3
DC-Chol-DOPE-FBS		360 ± 3	−11.4 ± 0
DC-Chol-DOPE/DNA		244 ± 4	48 ± 1.5
DC-Chol-DOPE/DNA-FBS		741 ± 1	−29.7 ± 0.2
DDAB-DOPE	0.7	114 ± 1	60.5 ± 1.3
DDAB-DOPE-FBS		1196 ± 300	−9.3 ± 0.4
DDAB-DOPE/DNA		296 ± 7	42.6 ± 0.2
DDAB-DOPE/DNA-FBS		2797 ± 500	−27.4 ± 1.3
DC-Chol-DOPE		105 ± 1	60.5 ± 1.3
DC-Chol-DOPE-FBS		1761 ± 400	−27.4 ± 0.7
DC-Chol-DOPE/DNA		211 ± 3	42.5 ± 0.2
DC-Chol-DOPE/DNA-FBS		2101 ± 700	−22.4 ± 0.5

Narrow particle size distributions (pdi = 0.2) show liposome suspensions to be monodisperse. When serum was added to liposomes, a significant increase in particle size was observed. Such an increase was found to be dependent on the charge density of lipid membranes and on lipid composition, with the former parameter having a more dominant effect. Liposomes at $\Phi = 0.5$ aggregated moderately, and serum caused a strong aggregation at increasing DOPE concentration ($\Phi = 0.7$). Many reports have shown that the higher the charge density, the more effective the protective effect against serum proteins.[31] As a result, the most compelling explanation for our observation is that, for higher membrane charge density ($\Phi = 0.5$), the neutralizing effect of serum is saturated by excess lipids. In that case, residual excess charge at the membrane surface prevents large aggregation and fusion of liposomes.

3.5. Effect of Serum on the Size of Lipoplexes. The size of lipoplexes was investigated to determine the importance of this parameter in transfection efficiency. According to Table 3, DC-Chol-DOPE/DNA lipoplexes in the absence of serum were ∼200 nm in size, whereas DDAB-DOPE/DNA complexes were ∼300 nm. In the presence of serum, the average dimensions of lipoplexes increased remarkably (Table 3), with a strong dependence on the membrane charge density of lipoplexes. Indeed, lipoplexes at $\Phi = 0.5$ were ∼740 nm in size, whereas complexes at $\Phi = 0.7$ were definitely larger than 1 μm. The particle size distribution shows lipoplexes at $\Phi = 0.7$ (data not reported) to be largely polydisperse.

In general, the similarity between the aggregation behavior of lipoplexes and free liposomes in their interaction with serum likely seems to confirm that the lipid bilayer is the primary target with which serum proteins interact.[32]

3.6. Effect of Serum on the ζ Potential of Liposomes and Lipoplexes. Previous studies showed that lipid vectors became negatively charged after exposure to serum.[3,4] Also, cationic lipid vectors recruited large amounts of serum proteins, particularly those containing DOPE as a helper lipid.[28] We measured the ζ potential, which is a widely accepted parameter for the physical characterization of particle surface charge, before and after the incubation of liposomes and lipoplexes in serum.

In the absence of serum, the ζ potential of lipid/DNA complexes was lower that that of free liposomes because of partial neutralization of the positive charge of cationic lipids by DNA. Following the addition of serum, we did not find large differences among formulations. The ζ potential of free liposomes reversed to slightly negative (∼ −10 mV), whereas it was definitely more negative in the case of lipoplexes (< −20 mV).

3.7. Effect of Serum on DNA Release from Lipoplexes. It has often been reported that serum caused lipoplexes to aggregate, resulting in DNA release and degradation. To find out whether interaction between serum components and lipoplexes is accompanied by lipid−DNA dissociation, we investigated the extent of DNA release by electrophoresis on agarose gels, which allows us to determine the molar fraction and conformation of DNA that is completely free from lipid. In Figure 9, we present the digital photograph of the four lipoplex formulations in the absence (lanes 1, 3, 5, and 7) and presence (lanes 2, 4, 6, and 8) of serum. Lane 9 is the control DNA. The high-mobility band was attributed to the most compact (supercoiled) form, whereas the less-intense one was considered to contain the nonsupercoiled content in the plasmid preparation. First, we observed that, in the absence of serum (lanes 1, 3, 5, and 7), the intensity of free DNA bands varied with membrane charge density and lipid formulation. Fixing the cationic lipid and increasing the molar fraction of DOPE (complexes at $\Phi = 0.7$) resulted in better DNA protection whereas at the same membrane charge density (i.e., at the same Φ) DC-Chol-DOPE/DNA lipoplexes exhibited a higher DNA-binding capacity than did DDAB-DOPE/DNA lipoplexes. The digital photograph in Figure 9 points to the existence of a large amount of free DNA in the DDAB-DOPE/DNA lipoplex formulation at $\Phi = 0.5$ (Figure 9, lane 1). The quantification of DNA (not reported) confirmed this observation. Approximately one-third of the DNA was found to be free and unprotected by DDAB-DOPE cationic liposomes at $\Phi = 0.5$.

After incubation with serum, there was no clear evidence of lipid−DNA dissociation (lanes 2, 4, 6, and 8). The intensity of free DNA bands remained roughly the same as its counterpart in the serum-free buffer. This implies that serum did not induce the dissociation of plasmid DNA from the cationic lipids. However, the presence of serum did strongly affect the conformation of unbound DNA. The free DNA topology in DDAB-DOPE/DNA lipoplexes at $\Phi = 0.5$ is shifted to an open-circular conformation (Figure 9, lane 2) compared to a predominantly supercoiled conformation in the absence of serum (Figure 9, lane 1).

The presence of serum did not affect the conformation of DNA protected by cationic lipids. This is visible after the release of DNA from lipoplexes by phenol−chloroform extraction (data not reported). Indeed, DNA extracted from DDAB-DOPE/DNA-FBS lipoplexes at $\Phi = 0.5$ is still present in a supercoiled conformation.

4. Discussion

Serum constitutes important barrier to cationic−lipid mediated gene transfer. The presence of serum in the transfection media has been found to be inhibitory to gene transfer.[7−9] This inhibition has been mainly attributed to serum proteins that can interact with lipid membranes. Degradation of the lipoplex structure is accompanied by lipid−DNA dissociation leading to a decrease in transfection efficiency. As a result, most studies have concentrated on improving the serum stability of lipoplexes and have clearly shown that maintaining intact lipoplexes in the presence of serum is important to retaining high transfection efficiencies.[33] At present, it is strongly believed that a better understanding of lipoplex structure and stability in serum is needed

(31) Madeira, C.; Loura, L. M. S.; Prieto, M.; Fedorov, A.; Aires-Barros, M. R. *BMC Biotechnol.* **2008**, *8*, 20–29.

(32) Chesnoy, S.; Huang, L. *Annu. Rev. Biophys. Biomol. Struct.* **2000**, *29*, 27–47.

(33) Cheung, C. Y.; Stayton, P. S.; Hoffma, A. S. *J. Biomater. Science* **2005**, *16*, 163–179.

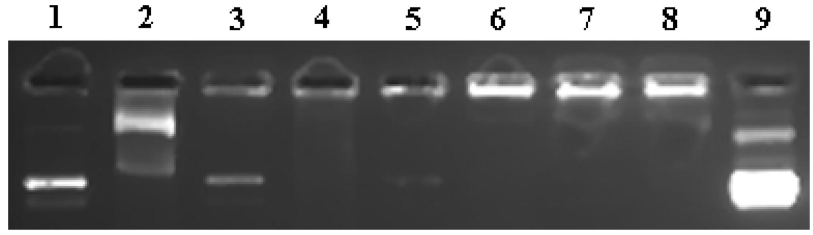

Figure 9. Digital photograph of the four lipoplex formulations in the absence or in the presence of serum: (lane 1) DDAB-DOPE/DNA lipoplexes at $\Phi = 0.5$; (lane 2) DDAB-DOPE/DNA-FBS lipoplexes at $\Phi = 0.5$; (lane 3) DDAB-DOPE/DNA lipoplexes at $\Phi = 0.7$; (lane 4) DDAB-DOPE/DNA-FBS lipoplexes at $\Phi = 0.7$; (lane 5) DC-Chol-DOPE/DNA lipoplexes at $\Phi = 0.5$; (lane 6) DC-Chol-DOPE/DNA-FBS lipoplexes at $\Phi = 0.5$; (lane 7) DC-Chol-DOPE/DNA lipoplexes at $\Phi = 0.7$; (lane 8) DC-Chol-DOPE/DNA-FBS lipoplexes at $\Phi = 0.7$; and (lane 9) control DNA. The high-mobility band was attributed to the most compact (supercoiled) form, and the less-intense one was considered to be the nonsupercoiled content in the plasmid preparation.

to clarify parameters that govern the mechanism of lipofection, thus providing tools for improving gene delivery.

In the absence of serum, all formulations tested in the present study were found to be fairly efficient (Figure 2) if compared to the highly efficient commercial Lipofectamine 2000 (Invitrogen) (data not reported). We considered the possibility that the nanostructural differences among formulations (Figures 3 and 4) could be responsible for their variable efficiencies. DC-Chol-DOPE/DNA lipoplexes at $\Phi = 0.5$ and 0.7 (Figure 3, panels a and b) were both organized in lamellar L_{α}^{C} phases with distinct DNA packing densities as a result of different membrane charge densities.[21,22] Also, DDAB-DOPE/DNA lipoplexes at $\Phi = 0.5$ were assembled into lamellar arrays (Figure 4, panel a), whereas DDAB-DOPE/DNA lipoplexes at $\Phi = 0.7$ exhibited the coexistence of lamellar and hexagonal phases (Figure 4, panel b). Numerous studies in search of a correlation between the structural properties of lipoplexes and their transfection efficiency have shown that lipoplexes that adopt the inverted hexagonal phase (Figure 1) are more fusogenic than lamellar, facilitate the intracellular release of DNA, and often display high transfection efficiency.[34,35] According to these suggestions, the superior efficiency of DDAB-DOPE/DNA lipoplexes at $\Phi = 0.7$ (Figure 2) may likely be related to their tendency to adopt such a bilayer-destabilizing inverted hexagonal phase.

Because the structure of the other three formulations did not correlate clearly with efficiency, we believe that parameters other than structure on the nanoscale level can modulate their transfection behavior. A number of physical−chemical properties of lipoplexes have been proposed as factors regulating transfection efficiency. In the present study, we investigated some physical−chemical characteristics that might account for the efficiency of lipoplexes, such as the size, surface potential, and DNA-binding capacity of cationic liposomes. In particular, the latter property of cationic liposomes, which is governed by the chemical nature of the amphiphile, has recently emerged as a critical factor controlling the transfection efficiency of lipid−plasmid complexes.[36,37] It is commonly accepted that efficient transfection will require an optimal protection of plasmid DNA by a coating of cationic lipid against degradation by DNA-ase enzymes in cells. Despite early convictions, recent findings have shown that mixing DNA and excess cationic lipid does not guarantee complete DNA complexation.[38]The optimization of cationic lipid/DNA complexes for transfection will require a determination of the optimal cationic lipid/DNA charge ratio necessary to complex the DNA completely.[38] These suggestions may help to explain why DDAB-DOPE/DNA lipoplexes at $\Phi = 0.5$ exhibited the lowest transfection efficiency among the formulations used in the present study.

Interestingly, serum increased the transfection efficiency of all lipoplex formulations (Figure 2, black histograms). The transfection efficiency of DDAB-DOPE/DNA at $\Phi = 0.7$ almost doubled in the presence of serum, whereas DDAB-DOPE/DNA at $\Phi = 0.5$ exhibited an approximate 4-fold increase. DC-Chol-DOPE/DNA lipoplexes exhibited intermediate increasing values.

The transfection capacity of numerous amphiphile formulations is affected by serum, but little is known about the underlying mechanism, with knowledge of this mechanism being a prerequisite for further development. In search of the reason that all lipoplex formulations exhibited such an increase in efficiency, we have examined the effect of serum on structural stability, DNA-protection capacity, particle size, and surface potential of lipoplex formulations.

The instability of lipoplexes in serum, which is one of the possible causes of the obtained lower transfection efficiencies, is a well-known phenomenon. To evaluate the stability of lipoplexes in serum, a comprehensive synchrotron SAXS study was performed. The multilamellar arrangement of DC-Chol-DOPE/DNA lipoplexes was maintained in serum (Figure 7, panels a and b). A characteristic structural feature was the swelling of the lamellar phase of lipoplexes in the presence of serum (Table 2) as a result of serum protein intercalation within lipid bilayers.

FBS does contain several blood proteins, including endonucleases. It was also suggested that there is a possibility that lipids of lipoprotein particles interact and fuse with cationic lipids. As a result, interaction between DNA and cationic lipids should be weakened, with the result that some DNA molecules can be released from lipoplexes. We observed that, upon addition of serum, interhelical DNA−DNA distances (Figure 7, panel c) remained essentially the same as their counterpart in the absence of serum (Figure 3, panel c). In recent papers, we have shown that DNA packing density (i.e., d_{DNA}) within lipoplexes[29,30] can be used to estimate the molar fraction of DNA released from lipoplexes by anionic molecules such as cellular lipids and proteins. Because the DNA packing density of lipoplexes was not affected by the presence of serum, we could therefore infer that, after incubation with serum, DNA was not released from lipoplexes and remained tightly bound to lipid bilayers. The latter observation most likely suggests that serum components did not penetrate into water layers occupied by DNA molecules but appeared to be associated mainly with the lipid membranes. Our structural findings are in fairly good

(34) Hui, S. W.; Langner, M.; Zhao, Y. L.; Ross, P.; Hurley, E.; Chan, K. *Biophys. J.* **1996**, *71*, 590–599.
(35) Zuhorn, I. S.; Oberle, V.; Visser, W. H.; Engberts, J. B.; Bakowsky, U.; Polushkin, E.; Hoekstra, D. *Biophys. J.* **2002**, *83*, 2096–2108.
(36) Simberg, D.; Danino, D.; Talmon, Y.; Minsky, A.; Ferrari, M. E.; Wheeler, C. J.; Barenholz, Y. *J. Biol. Chem.* **2001**, *276*, 47453–47459.
(37) Zuhorn, I. S.; Visser, W. H.; Bakowsky, U.; Engberts, J. B. F. N.; Hoekstra, D. *Biochim. Biophys. Acta* **2002**, *1560*, 25–36.
(38) Caracciolo, G.; Pozzi, D.; Caminiti, R.; Marchini, C.; Montani, M.; Amenitsch, H. *J. Appl. Phys.* **2008**, *104*, 014701–3.

agreement with the recent results by Madeira and co-workers,[31] who found evidence that this protein-induced fusion merely occurs at the lipoplex external layer and does not drastically affect the spacing distances between DNA molecules.

Synchrotron SAXS data indicated that serum promoted the lamellar-to-inverted hexagonal phase transition in DDAB-DOPE/DNA lipoplexes at $\Phi = 0.5$ (Figure 8, panel a). It has recently been proposed that serum protein intercalation within lipid bilayers can induce the formation of nonlamellar motifs in the membranes of lipoplexes.[6] To our knowledge, this is the first time that such a predicted phase transition has been reported. Even though providing a detailed explanation of our structural observation is not among the main goals of the present article, some qualitative arguments can be proposed. The ability of the lipoplex to adopt such an inverted hexagonal phase is dictated by a delicate interplay between electrostatic and membrane elastic interactions in the complexes.[23] Pure electrostatic interactions alone are expected to favor the inverted hexagonal phase, which minimizes the charge separation between the anionic phosphates on the DNA backbone and the cationic lipids, but they are opposed by the elastic cost of forming a cylindrical monolayer membrane around DNA. Mixing molecules within the lipid bilayer can reduce the bending rigidity of membranes and, in turn, can result in a reduction in the elastic energy barrier to the formation of the H_{II}^{C} phase.[23] Inverted hexagonal phases are proposed to play a key role in the endosomal escape of DNA and to display high transfection efficiency. Although we cannot exclude the fact that parameters other than the lipid phase could play a role in increasing the transfection efficiency mediated by DDAB-DOPE/DNA lipoplexes at $\Phi = 0.5$, the formation of the fusogenic inverted hexagonal phase may therefore be taken into account to explain why this formulation exhibited the highest increase in efficiency in the presence of serum.

The DNA-protection capacity of lipoplexes was not modified by serum. As can be seen in Figure 9, no migration of DNA into the agarose gels occurred. This indicates that serum did not induce the dissociation of plasmid DNA from the cationic lipids. This finding is in agreement with the structural results obtained by synchrotron SAXS experiments. Moreover, the presence of serum did not affect the conformation of DNA protected by cationic lipids. This is visible after the release of DNA from lipoplexes by phenol−chloroform extraction (data not reported). Indeed, DNA extracted from DDAB-DOPE/DNA-FBS lipoplexes at $\Phi = 0.5$ is still present in a supercoiled conformation. This finding indicates that the serum treatment of lipoplexes did not enhance nuclease accessibility. DNA was therefore completely protected by cationic lipids from nuclease activity. Conversely, free DNA was severely affected by serum, with topology being shifted to an open-circular conformation (Figure 9).

An important parameter of morphologies affecting transfection efficiency is lipoplex size. Although conflicting reports exist as to the optimal size of lipoplexes for lipofection, there is no doubt that large lipid particles guarantee maximum contact and fusion with cells.[39] In addition, large complexes taken up by cells lead to the formation of large intracellular vesicles that are more easily disrupted, easily release DNA into the cytoplasm, and transfect gene efficiently. Beside these aspects, it is strongly believed that the most significant role of lipoplex size is determining the nature of the entry pathway of complexes into the cells.[40] There is convincing evidence that endocytosis represents the major pathway of lipoplex entry into cells. However, various endocytic pathways exist in eukaryotic cells, with clathrin-dependent and caveolae-mediated internalization being the most relevant ones. Size appears to be an important parameter that (co)determines the mechanism of particle entry into cells. Recent studies have shown that lipoplexes with a size of 300 nm or less entered cells almost exclusively via the clathrin-coated pathway, whereas complexes larger than 500 nm are preferentially internalized via caveolae-mediated pathways.[40] Each of these pathways is biochemically different, and lipoplexes are processed differently in the cell. Most importantly, caveolae-mediated trafficking seems to avoid lysosomal digestion, which is supposed to contribute negatively to transfection. In addition, small serum protein-penetrated lipoplexes, being delivered to lysosomes prior to their ability to release their cargo from prelysosomal endocytic compartments, have been reported to be poorly efficient in vitro. In a recent study, it was shown that in CHO cells the transfection efficiency, cell association, and uptake of lipoplexes increased with increasing lipoplex size.[41] According to these suggestions, it has recently been claimed that only caveolae-mediated internalization can produce efficient transfection.[42]

Our data show that serum has a strong effect on lipoplex size (Table 3). In particular, in the absence of serum, lipoplexes are smaller than 300 nm, whereas in the presence of serum they are much larger than 500 nm. Consistent with the above-mentioned size-dependent entry mechanism, our data seemingly suggest that the transfection efficiency boost in serum (Figure 2) may likely be due to a serum-induced switch from clathrin-dependent to caveolae-mediated internalization. On the whole, we propose that structural stability and the increase in size rationalize the efficiency of lipoplexes in serum.

5. Conclusions

We have investigated the effect of serum on the nanometric structure, size, ζ potential, DNA binding capacity, and transfection efficiency of DC-Chol-DOPE/DNA and DDAB-DOPE/DNA lipoplexes as a function of the membrane charge density of cationic lipid membranes.

In the absence of serum, all tested formulations were found to be very efficient in trasfecting NIH 3T3 cells with varying efficacy, and this is mainly dependent on the lipid phase behavior and DNA-binding capacity of cationic liposomes.

Investigated lipoplexes were stable in serum, and no appreciable changes in lamellar structure and DNA packing density were detected. Neither DNA released from lipoplexes nor the morphology of DNA protected by cationic lipids was affected by serum. We believe that such a marked stability of tested lipoplex formulations in serum is a reasonable explanation of their efficiency. Major changes in lipoplex size were induced by serum. According to the established viewpoint of the size-dependent entry mechanism of lipoplexes, our results seemingly suggest that the increase in transfection efficiency in serum may be due to a serum-induced switch from a clathrin-dependent to caveolae-mediated mechanism of internalization of lipoplexes. If further confirmed, these results imply that, by controlling lipoplex stability and size in serum, an efficient lipid delivery system may be achieved.

Acknowledgment. We acknowledge Dr. T. Narayanan and Dr. E. Di Cola of the experimental staff of ID02 at ESRF for technical support. Professor Ruggero Caminiti is acknowledged for useful discussions.

LA8033726

(39) Koynova, R.; Tarahovsky, Y. S.; Wang, L.; MacDonald, R. C. *Biochim. Biophys. Acta* **2007**, *1768*, 375–386.

(40) Hoekstra, D.; Rejman, J.; Wasungu, L.; Shi, F.; Zuhorn, I. *Biochem. Soc. Trans.* **2007**, *35*, 68–71.

(41) Ross, P. C.; Hui, S. W. *Gene Ther.* **1999**, *6*, 651–659.

(42) Rejman, J.; Conese, M.; Hoekstra, D. *J. Liposome Res.* **2006**, *16*, 237–247.